

Electron Microscopy Protocols for the Study of Hydrocarbon-Producing and Hydrocarbon-Decomposing Microbes: Classical and Advanced Methods

Kamna Jhamb and Manfred Auer

Abstract

One of the fascinating areas of hydrocarbon microbiology biology is the quest for an ultratstructural understanding of (macro)-molecular mechanisms underlying the degradation, synthesis, and intracellular storage of hydrocarbons, which due to their hydrophobic characteristics continuously threaten the integrity of biological membranes. Here we review classical and novel advanced electron microscopy approaches, including correlative light and electron microscopy that in combination with genetics and biochemical experimentation can be utilized to study such hydrocarbon–cell interactions.

Keywords: Cellular inclusion, Correlative microscopy, Cryo-EM, Electron microscopy, Hydrocarbon, Lipid

1 Introduction

1.1 Significance

All life on Earth relies on the unique properties of water, and thus to carry out biochemical reactions efficiently, evolution has created lipid-enclosed membranes compartments, which allow (bio)chemical reactions to take place in a defined chemical environment. For this reason any lipophilic solvents, such as hydrocarbons, are of great danger to the integrity of these membranous compartments and thus to the integrity of its metabolism. It is therefore surprising that certain microorganism not only can exist in the presence of hydrocarbon but also can grow and strive under such conditions, using the high energy density stored in hydrocarbon to fuel their metabolism. Hydrocarbons are the Earth's most important natural energy resources, being the main constituents of petroleum and natural gas reserves. They are formed abiotically through pressure and appropriate temperature condition-mediated reduction of fossilized organic material such as zooplankton and algae in sediments. Petroleum and natural gas are critical to all human economic activities, including transportation, and energy and are therefore of high

geostrategic significance, and thus, any biotic mechanisms (e.g., caused by microorganisms residing in oil wells), by which such petroleum reservoirs may be affected, are of great importance to the petroleum industry. The very question by which mechanisms microorganisms can exist and even thrive in hydrocarbon-rich environment is fascinating, as it touches on tolerance toward presumably toxic chemical conditions and the microbial strategies employed to deal with the destabilizing effect of a lipophilic solvent. This question not only concerns the biodegradation of hydrocarbons but also the effective synthesis and storage of lipid moieties such as triacylglycerols (TAGs) and wax esters, which are used as storage reservoirs for energy, leading to the recognition of an entirely new branch of science called as “hydrocarbon microbiology.”

1.2 Hydrocarbon Microbiology

Certain systematic groups of microorganisms are characterized by specific composition of the hydrocarbon fractions; for instance, cyanobacteria are unique in their ability to produce 7- and 8-methylheptadecanes; photosynthetic bacteria are distinguished by the synthesis of cyclic hydrocarbons (pristane and phytane), whereas in fungi, long-chain hydrocarbons are predominant. It was assumed that the hydrocarbon composition of microorganisms could be used as a chemotaxonomic criterion. Microbial hydrocarbons appear to regulate the cell development; act as causative agents in the plant–microorganism, predator–prey, and interspecies interactions; and play an important ecological and physiological role [1].

There are at least four different aspects of hydrocarbon microbiology that go beyond an academic curiosity in hydrocarbon microbiology and thus are of industrial interest:

1. **Biodegradation of petroleum reserves:** Degradation of oil results in a decrease in its hydrocarbon content and an increase in oil density, sulfur content, acidity, and viscosity. These changes have negative economic consequences for oil production and refinery operations. Recent studies [2, 3] have concluded that in addition to aerobic bacteria in the shallow on-shore oil fields, a variety of anaerobic bacteria, including sulfate-reducing bacteria, iron oxide-reducing bacteria, and bicarbonate-reducing bacteria are capable of biodegrading oils. Most biodegrading organisms negatively impact the economics of the oil drilling process by generating carbon dioxide as a by-product when they degrade the hydrocarbons [4]. The knowledge of the microbiology of hydrocarbon degradation in petroleum reservoirs and of the microorganisms involved and the pathways by which these microbes utilize oil components as well as the conditions under which they thrive is critical and can save time for the exploration of new oil reserves [5].
2. **Bioremediation:** Oil spills that occur during drilling operations or other accidental oil spills are catastrophic for the fragile marine life in the affected areas. Microbes have long been

known to naturally degrade oil and its constituents [6]. The literature is filled with numerous reports and reviews, highlighting the exploitation of microorganisms for bioremediation [7–12]. Emergency response guidelines from the Environmental Protection Agency (EPA) for cleanup of oil spills consider biological agents (microorganisms) crucial for successful bioremediation approaches [13]. However, recently, Kostka and colleagues have highlighted the fact that despite the available advances in technologies for oil drilling, strategies to respond to oil spills and to assess environmental impacts of oil contamination have lagged behind. It is imperative that we develop a detailed understanding of the impacts of oil on indigenous microbial communities and pave the way for identification of oil-degrading microbial groups that are prerequisite for directing the management and cleanup of oil contaminated beach ecosystems [14].

3. **Biosynthesis of hydrocarbons:** Traditionally, hydrocarbon biomarkers have been used to constrain the age of the ancient bacteria, archaea, and eukaryotes owing to their long-term stability [1]. Gas and liquid chromatography as well as ultrastructural visualization by electron microscopy [15] has led to the discovery of intracellular hydrocarbons in microbes, which given the fact that microorganisms can be efficiently cultivated in bioreactors has led to a growing interest in using biotechnology for the production of fuels and chemicals, which to this date are largely derived from petroleum hydrocarbon reservoirs that are becoming scarcer and more expensive to exploit. Thus, it comes as no surprise that one goal of commodity biotechnology is to produce hydrocarbons via bacterial metabolism [16]. The major polymeric lipids produced by prokaryotes are poly (3-hydroxybutyrate) (PHB) or other polyhydroxyalkanoates (PHAs), whereas accumulation of triacylglycerols (TAGs) and wax esters (WEs) in intracellular lipid bodies is a property of only a few prokaryotes. The formation of PHAs, TAGs, and WEs is also promoted in response to stress imposed on the cells and during imbalanced growth, for example, by nitrogen limitation, if an abundant carbon source is present at the same time. All these lipids act as storage compounds for energy and carbon needed for maintenance of metabolism and synthesis of cellular metabolites during starvation [17–19]. The literature has since been growing on the studies conducted on the formation and mechanisms of hydrocarbon biosynthesis, accumulation, and transport in microbial cells [15, 16, 20, 21].
4. **Biofuels:** Ever-growing demands for crude oil and concerns about carbon emissions from fossil fuels contributing to the climate change and alternative renewable resources for transport fuel are urgently needed. Biofuels, in particular biodiesel,

which is produced from renewable biomass by transesterification of triacylglycerols, yielding monoalkyl esters of long-chain fatty acids with short-chain alcohols, for example, fatty acid methyl esters (FAMEs) and fatty acid ethyl esters (FAEEs), has gained considerable attention in this regard, even more so as it contributes no net carbon dioxide or sulfur to the atmosphere and emits less gaseous pollutants than normal diesel [22]. Plant oils and animal fats have been used to generate biodiesel worldwide. Ethanol, made mostly from corn starch from kernels, today is by far the most significant biofuel in the United States, accounting for 94% of all biofuel production in 2012. Most of the remainder is biodiesel, which is made from vegetable oils (chiefly soy oil) as well as animal fats, waste oils, and greases [23]. However, considering the economics of the production of biofuels and the amount of area required for cultivation of plants, researchers are now looking for other viable options. Oleaginous microorganisms such as yeasts, fungi, microalgae, and some bacteria are known to accumulate intracellular lipids, mainly triacylglycerols and some wax esters, which may prove to become promising alternatives [24]. Developing “high lipid content” microorganisms or engineered strains for biodiesel production would be becoming a potential and promising way in the future [22].

All the aspects of hydrocarbon microbiology discussed above highlight the need to understand microbial oil/lipid catabolism and anabolism and strategies for withstanding the solvent properties of these substances, threatening the integrity of cell membranes. Specifically, we would like to understand the exact mechanisms of biodegradation of oil and the microbial communities that are involved in this process and the synergistic behavior of community members. Also, we know very little about how the lipid inclusions/bodies accumulate inside the cell, their ultrastructure (shape and size), and how this process is controlled, as well as the transport mechanisms to and from the cell to extracellular medium. A combination of genetic, cell biological, biochemical, and biophysical (including ultrastructural) studies will yield insight on the cellular and molecular base of lipid bodies and the regulation of their accumulation and mobilization and thus could lead to the use of these organisms as a renewable energy resource [19, 25].

Direct imaging of hydrocarbons and lipids inside (or in the presence of) microorganism by light and electron microscopy allows the study of heterogeneous processes, where not all microorganism will contain the same amount of hydrocarbon and lipids, or where the hydrocarbons and lipids are found in (or are associated with) particular intracellular compartments. A few examples from our own research will illustrate the various approaches that are further detailed below. For example a variety of commercially available

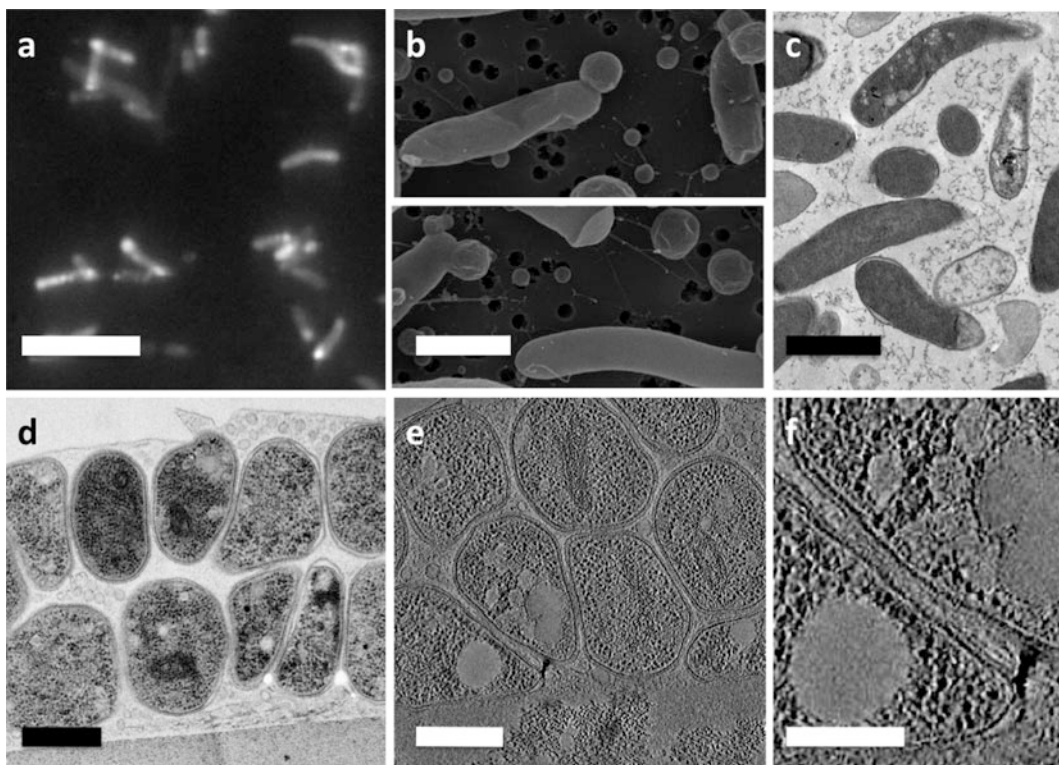


Fig. 1 Hydrocarbon/lipid storage in bacteria. Biodiesel producing *Escherichia coli* imaged by (a) fluorescence microscopy, revealing polar distribution of biodiesel, (b) scanning electron microscopy, showing ball-like structure most likely enclosing biodiesel, and (c) ultrathin-section transmission electron microscopy, revealing extracted polar regions. (d)–(f) High-pressure frozen, freeze-substituted *Myxococcus xanthus* biofilms as imaged by transmission electron microscopy of 100 nm ultrathin sections (d). Upon 3D imaging by electron tomography, single or merged drop-like empty compartments and their ultrastructural relationship to the bacterial cytoplasm can be studied in 1 nm slices of the 3D tomograms in exquisite detail. Scale bars: $a = 5 \mu\text{m}$; $b = 1 \mu\text{m}$; $c = 1 \mu\text{m}$; $d = 500 \text{ nm}$; $e = 500 \text{ nm}$; $f = 250 \text{ nm}$

lipophilic dyes can be used to visualize such hydrocarbon and lipid distributions, e.g., when screening biodiesel-producing bacteria (Fig. 1a). Such biodiesel-producing bacteria can also be visualized for unusual morphology using scanning electron microscopy (SEM) revealing ball-like objects emerging typically at the poles of the bacterial cells (Fig. 1b) or transmission electron microscopy (TEM), where the pole regions are often found depleted of material due to hydrocarbon extraction during lengthy sample preparation (Fig. 1c). Hydrocarbon deposits can be visualized also in biofilms using 2D (Fig. 1d) and 3D TEM (Fig. 1e,f) as the absence of material in resin-embedded samples that have been faithfully preserved by ultrarapid freezing and freeze substitution (see below). A close-up look reveals that such “empty” compartments that contained hydrocarbons prior to freezing are not bound by a membrane but appear like an oil-drop in a watery emulsion, sometimes

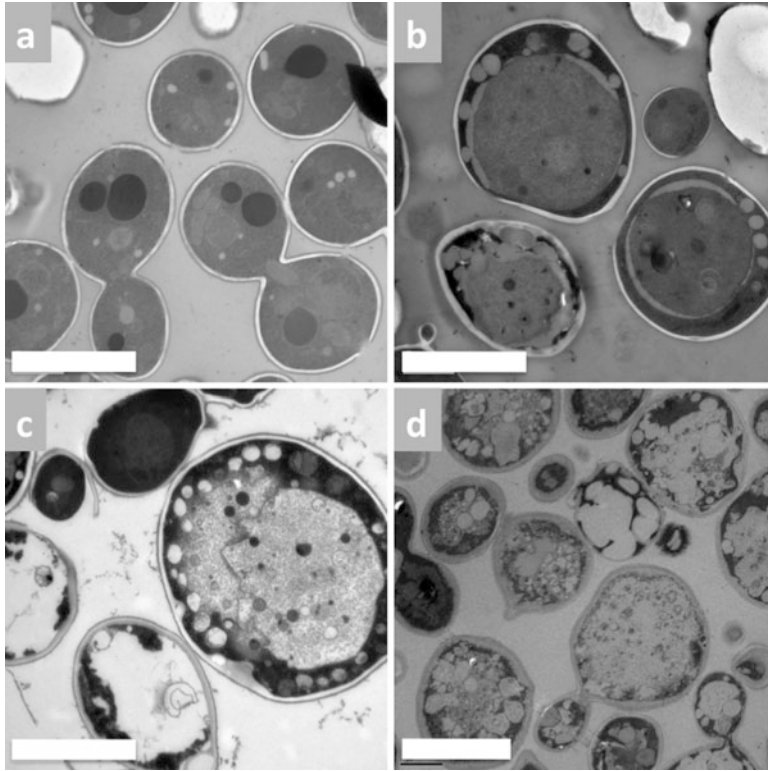


Fig. 2 Hydrocarbon-producing yeast (*Saccaromyces cerevisiae*). (a) Wild-type yeast strain prepared by high-pressure freezing and freeze substitution. (b)–(d) Yeast strain producing increasing amounts of hydrocarbons. Note the increasing number and size of droplet-like compartments, indicating the location of hydrocarbon prior to extraction. Scale bars: 5 μm

with several of such droplets partially merging, resulting in deviations from a simple ball-like geometry (Fig. 1f). Ultrastructural characterization of yeast cells producing different amounts of hydrocarbon (Fig. 2) not only reveals an increased amount of hydrocarbon production but also reveals the effect such increased hydrocarbon production has on cellular morphology and architectural organization. Cells that produce a high titer are often found to be abnormally shaped and appear highly stressed (Fig. 2d), compared to cells with moderate (Fig. 2c), low (Fig. 2b), and no (Fig. 2a) hydrocarbon production.

Resin section electron microscopy yields high-resolution ultrastructural information not visible by other means, leading to the discovery of intracellular lipid bodies [15, 26], which are formed in methane-utilizing bacteria and other hydrocarbon-utilizing bacteria and have been found in a variety of microbial species: Only hydrocarbon-grown *Acinetobacter* sp. cultures possessed intracellular lipid inclusion bodies [27]. Hydrocarbon-degrading *Rhodococcus opacus* strain PD630 possesses electron-transparent inclusions, the fatty acid composition of which depended on the substrate used [28]. Ultrathin sections of the strain DE2007 grown in the

presence of crude oil showed highly electro-dense (HE) inclusions of different sizes distributed throughout the cytoplasm of the bacterium [29]. Similarly, microbodies that have a homogeneous matrix and are surrounded by single unit membranes appeared profusely in various strains of *Candida* yeasts grown in *n*-alkanes. For a detailed review of the electron microscopic methods used for visualization of hydrocarbon-utilizing yeasts, see [30].

Traditionally, *osmium tetroxide* (OsO_4) is used as the major contrasting agent as it reacts with the carbon-carbon double bonds of unsaturated polymers, therefore staining the polymer and also fixing it in place, chemically cross-linking the sample, and causing hardening and increased density [31]. Wigglesworth as early as 1957 showed that tissues fixed with osmium tetroxide and then treated with ethyl gallate aided essentially in visualization of lipids since un-denatured proteins take up relatively little osmium, and nucleic acids and carbohydrates are completely unreactive [32]. Contrast of lipid-rich structures can be further enhanced by a saturated solution of monoterpene hydrocarbon myrcene, with or without the addition of 0.1% ethyl gallate in 70% ethanol, followed by osmium tetroxide, which allowed the visualization of both saturated and unsaturated lipids, including waxes [32]. Since osmium tetroxide will react predominantly with unsaturated lipids, Trent introduced *ruthenium tetroxide* (RuO_4) as a far more vigorous oxidant than OsO_4 to stain both aromatic and unconjugated unsaturated organic compounds, as well as some unsaturated polymers [33], which allowed visualization of microphase-separated saturated hydrocarbon diblock copolymers [34]. After this contrast-generating step, samples are typically dehydrated in either a graded ethanol or acetone series, with less lipid loss typically being observed when acetone was used instead of ethanol.

Freeze-fracture electron microscopy is a powerful technique that has revolutionized our understanding of lipid structures, although it is rarely used these days. The hydrophobic fats and oils are non-etchable unlike water-containing materials, and therefore in freeze-fractured specimens, they can be readily recognized after etching. Frequently one encounters non-crystallized, lipid droplet-like fats in biological samples, which appear amorphous, e.g., droplets of olive oil [35] or lipid droplets (chylomicrons) in the human blood [36] in contrast to lipid granules (fat droplets) in yeast cells, which appear as laminated structures [37, 38].

Freeze etching, a variant of the freeze-fracture approach, has enabled the viewing of cells without prior chemical treatment, thereby avoiding the potential artifacts encountered in processing specimens for resin embedding and ultrathin sectioning, and has provided evidence for the presence of a smooth-surfaced limiting membrane for the hydrocarbon inclusions [39]. In another study, freeze-fracture studies demonstrated the presence of the rectangular intracellular inclusions and intracytoplasmic membranes in hexadecanol-grown cells of *Acinetobacter* sp. [17].

Quick-freezing replica microscopy was employed as a tool to study the structure of the disk-shaped inclusion bodies in *Acinetobacter* sp. strain M-1 cells, which had a smooth surface, and grew to almost the same diameter as the cells. However, in this case no intracytoplasmic membrane structures or limiting membranes surrounding these inclusions were observed [40]. It is worth noting that although this approach offers a complementary perspective to thin-section analysis, one does not image the native structure but a metal replica of the fractured surface, with metal decoration artifacts having been described, making freeze-fracture images not always easy to interpret [41]. Another limitation of the freeze-fracture technique is the need to identify the chemical nature of the structural components visualized. Thus the combination of cytochemistry with freeze fracture led to the introduction of a new method called as freeze-fracture replica immunolabeling technique (FRIL) [42]. In this technique, samples are frozen, fractured, and replicated with platinum carbon as in standard freeze fracture and then carefully treated with sodium dodecylsulfate to remove all the biological materials except a fine layer of molecules attached to the replica itself. Immunogold labeling of these molecules permits their distribution to be seen superimposed on high-resolution planar views of membrane structure, leading an improved understanding of lipid droplet biogenesis and function [43, 44].

Negative-stain electron microscopy employing phosphotungstic acid as a rapid and simple technique allows the visualization of hydrocarbon inclusions in bacterial cells and their membrane fractions [27, 45], permitting the study of morphology of these particles albeit the danger of artifacts such as a rouleau forms in lipid-bound forms of apoE4 persists.

1.2.1 Water-Compatible Durcupan Resin Infiltration

Conventional electron microscopy sample preparation methods can lead to the loss of osmicated hydrocarbon bodies during organic solvent-based dehydration and epoxy resin embedding, leaving behind electron-lucent halo [27, 41, 46]. However, hydrocarbon inclusions, e.g., in alk-1-ene grown bacteria, were retained by employing water-compatible infiltration (water-Durcupan graded series) procedures [27]. Durcupan infiltration of hexadecane-grown cells has been shown to minimize extraction of the hydrocarbon, whereas the remainder of the cellular ultrastructure appeared similar to ethanol-dehydrated cells, with the interesting finding that hexadecane inclusions often appeared membrane bound in the Durcupan-infiltrated cells [39].

1.2.2 Advanced EM Imaging Approaches

Apart from the more traditional imaging approaches, some less commonly used and/or newer and thus more advanced imaging approaches have been applied to hydrocarbon microbiology, including cryogenic sample preparation and correlative light and electron microscopy approaches:

1.2.3 High-Pressure
Freezing–Freeze
Substitution (HPF–FS)

Ultra-rapid freezing followed by low-temperature dehydration has long been recognized as resulting in significantly improved cellular ultrastructure [47–49] by immobilizing within milliseconds the cellular scenery and subsequently gently replacing the cellular water ice by an organic solvent, thus circumventing a variety of macromolecular aggregation and extraction artifacts typically encountered during conventional sample processing. After vitrification, the sample can either be freeze-substituted, resin embedded prior to room-temperature ultrathin sectioning, or sectioned (cryo-ultramicrotomed) directly in its frozen-hydrated state [50], an approach (CEMOVIS) that is technically extremely challenging and thus not well suited for most investigators not specialized in this technique. Using freeze substitution, Paul and Beveridge [51] demonstrated that OsO_4 provides strong covalent interaction with the lipids preventing their leaching during the solvent washes.

1.2.4 Cryo-Electron
Microscopy of Vitreous
Sections (CEMOVIS)

In this approach that is only mastered in a handful or two of labs in the world and is technically quite challenging, sample are often vitrified by high-pressure freezing and cryo-sectioned in their frozen-hydrated state instead of freeze substitution and resin embedding [52]. Apart from the technical challenge to cut ultra-thin sections from a frozen block surface at liquid-nitrogen temperature and to effectively transfer the frozen section to an electron microscope grid with an eyelash in the absence of a solvent onto which the section could be floated and to make the sections stick to the grid without melting and/or drying out of the section, there are a variety of issues such as compression artifacts that render this approach somewhat limited to a more general set of scientists.

1.2.5 Tokuyasu
Sectioning

In this approach the sample is typically infiltrated by comparatively high concentrations of sugar, which acts like a cryoprotectant and also as an agent to mitigate any effects from drying by providing a hydration shell and possibly the retention of small amounts of water during the drying out of the sections. The advantage over CEMOVIS is that this approach is relatively easy and robust and allows (together with the HPF–FS approaches) immuno-affinity labeling.

A systematic study was carried out where different protocols, including (1) conventional, (2) Tokuyasu cryo-sectioning, (3) HPF–FS with room-temperature epoxy resin embedding, (4) HPF–FS with low-temperature Lowicryl HM20 embedding and ultraviolet (UV) polymerization, as well as (5) cryo-electron microscopy of vitreous sections (CEMOVIS), were tested for the visualization of *Mycobacterium smegmatis* cell structures along with lipid bodies [41]. HPF–FS avoided the artifacts encountered by conventional protocols, but displayed difficulties to visualize the monolayer boundary of the lipid bodies, which could be detected by CEMOVIS and which are thought to exist (*see* [19]).

1.2.6 *Whole-Mount
Cryo-Electron Microscopy
(Cryo-EM)*

Cells smaller than about 0.5–1 μm in diameter can be vitrified by plunge freezing into liquid ethane and studied as whole-mount samples, circumventing the need for organic solvents, resin, and ultrathin sectioning, thus allowing the entire cells to be imaged in their native frozen-hydrated state. This approach is widely considered as the gold standard for transmission electron microscopy imaging and upon 3D tomographic imaging can yield unprecedented insight into the bacterial large macromolecular complexes and organelles, such as PHA and polyphosphate inclusions in *Caulobacter crescentus* [53]. However, cryo-EM is technically demanding, including rapid plunge-freezing sample vitrification to avoid freeze-damage, liquid-nitrogen temperature grid handling to avoid contamination, as well as low-dose cryo-EM imaging, rendering this technique beyond the scope of this chapter.

1.2.7 *Wet Scanning
Transmission Electron
Microscopy*

A rather new and somewhat exotic approach is the use “wet scanning transmission electron microscopy” (STEM) to study polyhydroxyalkanoate and triacylglycerol carbon storage inclusions in bacterial cells [54]. Sample preparation is relatively fast and uncomplicated as only cooling to $\sim 1^\circ\text{C}$ during imaging is required. Given their lower density compared to the cytoplasm, hydrocarbon inclusions (PHA and TAG) are readily observed as relatively electron-lucent inclusions within cells, demonstrating the utility of wet STEM for imaging such structures without staining albeit at somewhat poor resolution compared to traditional TEM methods.

1.2.8 *Correlative Light
and Electron Microscopy
(CLEM)*

While the approaches above mostly rely on direct ultrastructural detection of the inclusions, correlative light and electron microscopy approaches allow the visualization of the dynamics of cellular hydrocarbon inclusions followed by ultrastructural analysis, either through image registration or via photoconversion, where the fluorescence signal is turned into an osmiophilic precipitate. Both Nile Red and BODIPY FL have been employed as lipophilic fluorophores. *Nile Red*, a phenoxazine dye, is almost nonfluorescent in water and other polar solvents but undergoes fluorescence enhancement and large absorption and emission blue shifts in nonpolar environments [55]. Nile Red has previously been used to screen bacteria, cyanobacteria, and microalgae for those producing fatty acids and esters [56]. A high-throughput method for detection of bacterial hydrocarbons in the form of PHA inclusions using Nile Red fluorescence was described recently [16]. *BODIPY 505/515* (4,4-difluoro-1,3,5,7-tetramethyl-4-bora-3a,4a-diaza-s-indacene) is a highly lipophilic neutral fluorophore used to label a wide range of hydrophobic compounds such as fatty acids, phospholipids, cholesterol, cholesteryl esters, and ceramides [57] and has been used to evaluate lipid droplets in microalgae [58]

determine cellular localization of bacterial lipids [21]. Fluorophores that can be bleached are well suited for correlative light and electron microscopy through *photooxidation of diaminobenzidine* (DAB) that results in the formation of brown DAB precipitate that is osmiophilic and thus readily visible at the electron microscopic level [59, 60]. Lipid prebodies of *R. opacus* PD630 were found after DAB photoconversion of BODIPY FL C₁₂-stained cells to correspond to the observed peripheral lipid domains observed in fluorescence microscopy [21].

1.2.9 Possible Future Directions

Not currently exploited very much, but potentially very interesting, is the correlative optical spectral data imaging (Fourier transform infrared spectroscopy or Raman microspectroscopy) with ultrastructural imaging, as the former is nondestructive and sensitive to chemical nature of the hydrophobic compounds and thus can be applied prior to the somewhat destructive electron microscopy imaging. This combination of chemical specificity with ultrastructural architectural sensitivity could prove to be of high value to the increasingly interesting and important field of hydrocarbon microbial research, but their synergy has yet to be demonstrated.

2 Materials

2.1 Preparation of Hydrocarbon-Grown Microbial Cells for Standard Transmission Electron Microscopy (TEM)

2.1.1 Primary Fixation (Use Electron Microscopy or Analytical-Grade Reagents)

1. Electron microscopy grade glutaraldehyde, 2.5%:

CAUTION: Fixatives are poisonous irritants; work in a fume hood and wear gloves.

Glutaraldehyde fixatives are easily prepared from 25% solutions of electron microscopy grade glutaraldehyde in sealed ampoules by making a 1:10 dilution in the buffer of choice.

To make 100 mL of 2.5% glutaraldehyde with 0.1 M CaCl₂:
 50 mL 0.2 M buffer stock solution at proper pH
 10 mL 25% glutaraldehyde (electron microscopy grade)
 2 mL 0.1 M CaCl₂ (IMPORTANT: do not use CaCl₂ with phosphate buffer as a precipitate will form)
 40 mL distilled water

2. Sodium cacodylate ((NaCH₃)₂AsO₂·3H₂O) buffer (0.2 M):

CAUTION: Cacodylate buffer contains arsenic and poisonous, carcinogenic substances that can be absorbed through the skin; wear gloves.

Cacodylate buffer consists of a 0.2 M stock solution of sodium cacodylate in distilled water (4.28 g/100 mL) and the pH is adjusted by adding the appropriate volume of 0.2 M HCl (1.7 mL concentrated HCl/100 mL distilled water) to the 100 mL stock as shown in Table 1.

Table 1
Preparation of cacodylate buffer (0.2 M)

pH	6.2	6.4	6.6	6.8	7.0	7.2	7.4
0.2 M HCl, mL	47.6	36.6	26.6	18.6	12.6	8.4	5.5

Table 2
Preparation of PBS (0.1 M, pH 7.3)

Reagent	Formula weight	Quantity	Final concentration
Sodium chloride (NaCl)	58.44	80 g	1.37 M
Potassium chloride (KCl)	74.56	2 g	26.8 mM
Sodium phosphate (Na ₂ HPO ₄)	142	14.2 g	0.1 M
Potassium phosphate (KHPO ₄)	136.1	2.4 g	17.6 mM
Hydrochloric acid (HCl), 1 N	NA	NA	1 N

To 100 mL of 0.2 M cacodylate solution (4.28 g/100 mL distilled water), add the appropriate amount of 0.2 N HCl (1.7 mL concentrated HCl/100 mL distilled water) to obtain the desired pH.

3. Phosphate-buffered saline (PBS):

Dissolve the chemicals listed in Table 2 in 800 mL of distilled water by stirring in a beaker.

Adjust pH to 7.3 with 1 N HCl.

Transfer to a graduated cylinder and adjust volume to 1 L with distilled water.

Sterilize by filtering through a 0.2- μ m filter flask or autoclaving.

2.1.2 *Washing*

1. 5% w/v sucrose: Dissolve 5 g per 1 L of the buffer used. Adjust the weight of sucrose required accordingly, such as, for 100 mL of buffer used, dissolve 0.5 g of sucrose.

2.1.3 *Postfixation*

1. Osmium tetroxide (OsO₄), 1%:

CAUTION: Osmium tetroxide is toxic, and the volatile fumes are very corrosive, especially to mucous membranes. It is essential that osmium solutions are handled in a fume hood and used osmium solutions be disposed of properly.

Prepare a 2% aqueous solution (1 g of osmium tetroxide in 50 mL of distilled water). A working fixative of 1% is prepared

just before use by mixing equal parts of 2% aqueous stock osmium tetroxide solution with an equal part of 0.2 M buffer.

2.1.4 Embedding of Cells in Agar Blocks (Optional)

1. Noble agar, 2%: Noble agar is the highest purity agar available. It is obtained after being washed in accordance with the Noble and Tonney method which removes trace impurities, ash, and minerals that interfere with many sensitive applications. To prepare, weigh 2 g of agar in 100 mL of distilled water or buffer. Bring to a boil and heat until it completely dissolves. Bring down the temperature to about 45°C and then pour desired amount over the bacterial cells. Allow to solidify without disturbing the tube.

2.1.5 Dehydration Series

1. Ethanol–water series:

CAUTION: flammable

Prepare 30, 50, 70, 90, 96% v/v ethanol in distilled water according to Table 3.

Keep 100% (absolute) ethanol in sealed pint containers.

2. Durcupan–water series:

CAUTION: Take great care when working with Durcupan, as this substance may cause skin irritation and allergic reactions. Work always with rubber gloves.

Durcupan, a water-soluble epoxy resin produced by the Fluka subsidiary of Sigma-Aldrich, is commonly used for embedding electron microscope samples. However, from the perspective of this paper, the employment of Durcupan dehydration has been shown to minimize extraction of the hydrocarbon in the preparation of specimens for thin sectioning [39]. The recipe for dehydration series containing component A (a water-soluble aliphatic polyepoxide) with water can be prepared as mentioned in Table 4.

Table 3
Preparation of ethanol–water dehydration series for 100 mL final volume

Volume of ethanol (mL)	Volume of water (mL)	Final % of ethanol
30	70	30
50	50	50
70	30	70
90	10	90
96	4	96

Table 4
Preparation of Durcupan–water dehydration series for 100 mL final volume

Volume of Durcupan (component A) (mL)	Volume of water (mL)	Final % of Durcupan
50	50	50
70	30	70
90	10	90

2.1.6 Embedding Resins

CAUTION: Both are hyper-allergenic and VCHD is carcinogenic.

1. Epoxy resin 812: Epoxy resin 812 consists of epoxy resin (originally designated Epon 812), the hardeners dodecenylsuccinic anhydride and methyl nadic anhydride, and an accelerant such as benzyltrimethylamine (BDMA) or 2,4,6-tris(dimethylamino-methyl) phenol. Prepare epoxy resin 812 embedding medium by pouring measured amounts (usually volumes) into a graduated, disposable polypropylene tube such as a 50 mL centrifuge tube with a tight-sealing cap. A mixture of medium hardness consists of the following components:

Epoxy resin 812 20 mL (24.0 g)

Dodecenylsuccinic anhydride 16 mL (16.0 g)

NMA 8 mL (10.0 g)

BDMA 1.3 mL (1.5 g)

Mix the resins thoroughly to obtain satisfactory results by inverting the tube end over end for 5–10 min.

2. Spurr's resin: The classical formulation of Spurr's resin consists of vinylcyclohexene dioxide (VCHD) or another cycloaliphatic epoxide ERL-4221, diglycidyl ether of polypropylene glycol (DER 736, Dow Epoxy Resin 736), nonenylsuccinic anhydride, and an accelerant such as BDMA or dimethylaminoethanol. Spurr's embedding medium is prepared by weighing components in a 50 mL graduated centrifuge tube on a top-loading balance. Prepare Spurr's resin of firm hardness resin as follows:

VCHD (or ERL-4221) resin 10.0 g

DER 736 6.0 g

Nonenylsuccinic anhydride 26.0 g

Dimethylaminoethanol 0.4 g

In order to prepare the mixtures of resin–water, mix thoroughly the appropriate volume of resin and water in 50 mL polypropylene tubes, and keep them capped until needed.

2.1.7 Staining

CAUTION: Uranium compounds are toxic and radioactive. Contact your safety officer or local authorities for appropriate handling and disposal protocols.

1. Uranyl acetate, 1%: Weigh 0.1 g uranyl acetate and dissolve in 10 mL of pre-warmed distilled water in a polypropylene tube and mix until all the crystals dissolve. Make aliquots by filtering through a 0.22 μ syringe filter and store them in dark at 4°C.
2. Lead citrate:
Place 1.33 g lead nitrate and 1.76 g sodium citrate into a 50 mL volumetric flask and add 30 mL water. Shake vigorously for 1 min. Allow to stand at room temperature for 30 min with intermittent shaking. Solution will be a milky white color. Add 8.0 mL of 1 N sodium hydroxide and mix. Solution will turn clear. Make up to 50 mL with boiled, cooled, and filtered double-deionized water. Store in a tightly sealed volumetric flask. Seal stopper with Parafilm. Do not use until the following day.

2.2 Preparation of Microbial Cells for Visualization by Negative Staining

1. Phosphotungstic acid, 1.5%:
Dissolve 1.5 g phosphotungstic acid in 100 mL distilled water. Adjust the pH to 7.0 with KOH. Store at 2–8°C.

2.3 Preparation of Microbial Cell Samples for High-Pressure Freezing–Freeze Substitution (HPF–FS)

1. Microbial cells resuspended in hexadecane
2. Membrane carriers (100 μ m deep, Leica) coated with 100 mg/mL lecithin (dissolved in chloroform), dried
3. High-pressure freezer (Leica EMPACT2-RTS, Leica Microsystems, Vienna, Austria)
4. Freeze-substitution medium: 1–2% osmium tetroxide (OsO_4) plus 0.5% uranyl acetate (UA) in acetone
5. Cryovials with o-ring seal (Genesee Scientific)

2.3.1 Quick Freeze Substitution Method: Preparation of Microbial Cell Samples for High-Pressure Freezing–Quick Freeze Substitution (HPF–QFS)

1. A modular heating block with 13 mm holes (VWR International, PA).
2. A foam box of dimensions (15 cm W \times 11 cm D \times 8 cm H, approx.) filled with liquid nitrogen. Walls of the box were around 2.5 cm thick.
3. A type T thermocouple temperature probe wrapped around a cryovial filled with 1.5 mL acetone and connected to a data-logger. Place it in one of the holes of the heating block.

2.4 Diaminobenzidine (DAB) Photoconversion

1. Fluorescent staining solution:
Prepare DMSO stock solution of 0.5 mg/mL Bodipy FL C12 (Molecular Probes, United States).
2. Primary fixative:

- 2% (w/v) paraformaldehyde and 0.5% (w/v) glutaraldehyde in PBS.
3. Chilled 0.5 mg/mL DAB solution in PBS
 4. Conventional fluorescence microscope with a fluorescein filter setting (BP530-560), a 50 W mercury lamp, and a 10X objective.
 5. Postfixative:
1% (w/v) OsO₄ in PBS (use caution while using osmium tetroxide)

3 Methods

3.1 Preparation of Hydrocarbon-Grown Microbial Cells for Standard Transmission Electron Microscopy (TEM)

The protocol described below is a general method for visualization of lipid bodies in microbial cells in particular, bacteria. Hydrocarbon microbiology has been gaining importance from the point of view of biofuel production or exploitation of microorganisms for bioremediation. In either scenario, visualization of accumulated lipids can provide an insight into the mechanisms of hydrocarbon metabolism, the pathways to its degradation, or the complex transport mechanisms involved. This protocol is a compilation of several protocols and should be optimized for best conditions.

3.1.1 Primary Fixation

Exponential-phase hydrocarbon-grown microbial cells are fixed in glutaraldehyde alone (2.5–6.25%) or containing calcium chloride (*see Note 1*) in a suitable buffer for 45 min to 1 h at room temperature. The buffer employed is generally sodium cacodylate (0.01–0.2 M, pH 7.2) or PBS (0.1 M, pH 7.3).

1. Pellet the cells by centrifuging at 7,000–10,000 rcf (*see Note 2*) for 5–10 min and remove most of the culture medium using a pipette.
2. Fix the cells by adding an excess volume (5–10 times the cell volume) of fixative and resuspend the cells in the fixative. A wide-bore pipette can be employed to gently resuspend the cells.
3. Incubate at room temperature for 45 min to 1 h with gentle shaking on a rotary shaker.
4. The cells are then pelleted in a microfuge tube (3–5 min at max rpm). Fixative removed. Leave a few drops in the cells so that they do not dry up.

3.1.2 Washing

Fixed cells should be washed in distilled water or more preferably in the same buffer that was used in the primary fixation step. Washing should be as thorough as possible, at least three times, each step for 20 min. Five percent wt/vol sucrose can also be added to the buffer in this step.

1. For the first washing step, resuspend the cells in ten times the cell volume of washing buffer or distilled water and shake gently on a rotary shaker for 20 min.
2. Pellet the cells by centrifugation at max speed for 5 min.
3. Resuspend the cells in the washing buffer and shake gently for 20 min.
4. Repeat the centrifugation and rinsing with the buffer at least one more time.
5. Finally pellet the cells for addition of postfixative.

3.1.3 Postfixation

The cells are then postfixated with 1.0% osmium tetroxide in the same buffer that was used in first fixation step (i.e., either PBS or cacodylate) for 90 min.

1. To the cell pellet, add 1% buffered osmium fixative and incubate for 90 min at room temperature, in the dark.
2. Carefully collect the cells by centrifugation.

3.1.4 Washing

The cells are again washed at least three times in the appropriate buffer (0.1 M cacodylate or PBS) by following the steps listed in Sect. 3.1.2.

3.1.5 Embedding of Cells in Agar Blocks (Optional)

The fixed cells are suspended in 2.0% (wt/vol) noble agar. Agar blocks (1 mm³) containing fixed cells are then further processed. It is important that the cell pellet is loose for this step.

1. Using a warmed plastic pipette (*see Note 3*), quickly transfer a few μL of warm agar onto the loose cells and gently stir the cells with the tip of the plastic pipette to suspend the cells in the warm agar. Do not dilute the cells in the agar.
2. Let the agar solidify. Do not touch or disturb the tube during the solidification process, or it will not harden properly.
3. Very carefully cut open the tube using a sharp razor blade to remove the agar plug containing cells.
4. Transfer them in a petri dish containing buffer and trim the agar into 1 mm cubes using a sharp razor blade.

3.1.6 Staining (Optional)

En bloc stain with 1% aqueous uranyl acetate (UA) for ~2 h at 4°C IN DARK (must be carried out in the dark as UA is photoreductive and will precipitate).

3.1.7 Dehydration

From the perspective of hydrocarbon visualization, Durcupan dehydration of hexadecane-grown cells has been shown to minimize extraction of the hydrocarbon in the preparation of specimens for thin sectioning [39]. The routine followed by Staubli (1963) was Durcupan–water series (50, 70, and 90% Durcupan, each step

for 15–30 min; two changes of 100% Durcupan, each step for 30–60 min) [61].

However, ethanol–water dehydration has also been routinely employed.

1. Dehydrate the cell pellet/cubes in graded water – ethanol series (30, 50, 70, 90, 96, and 100% ethanol) each step for 15 min.
2. Follow up with three changes of absolute ethanol, 10 min each. In case embedding medium to be used is epoxy resin 812, further perform three changes of propylene oxide (*see Note 4*), each for 15 min.
3. Remove most of the propylene oxide from the specimen cubes but leave a trace to prevent the cells from drying out.

3.1.8 Resin Embedding

A number of resins have been employed in the literature such as Spurr [21], Vestopal [26], Epon Araldite [17], epoxy resin 812, and Maraglas [27]. However, the most commonly used resins have been Spurr and epoxy resin 812, the methods for which have been described below. Spurr's embedding medium is recommended for bacterial cells since it infiltrates the bacterial cells better than epoxy resin 812. It has been suggested that to extend the times in the propylene oxide: Spurr's resin mixtures to 2 h each and the pure Spurr's resin mixture to overnight. Keep the capsules capped since this resin will absorb moisture and give an improper polymerization.

1. Prepare three mixtures of absolute ethanol: epoxy resin 812 embedding medium consisting of 3:1, 1:1, and 1:3 parts, each in 10 mL of graduated, disposable polypropylene tubes with tight fitting lids. Care should be taken to avoid air bubbles while mixing (*see Note 5*).
2. After the final change of absolute ethanol, gently pour on the 3:1 mixture of absolute ethanol/epoxy resin 812 embedding medium. Gently swirl the culture vessel five to six times over a period of 60 min to assist infiltration of the mixture into the cells. Similarly, repeat this procedure with the 1:1 and 1:3 mixtures.
3. Finally add pure epoxy resin 812 embedding medium and let it infiltrate for 60 min. Repeat this step one more time.
4. Replace the second epoxy resin 812 embedding medium with one final change and leave overnight, uncovered to facilitate evaporation of any residual ethanol.

A suggested infiltration schedule for Spurr resin in case of Durcupan–water dehydration method is Durcupan–Spurr (50:50, v/v), 5 h; Durcupan–Spurr (25:75, v/v), 8 h; and 100% Spurr, 5 h (twice) [39].

3.1.9 Polymerization

Polymerize epoxy resin 812 embedding medium for 48 h at 60°C. Polymerization of Spurr can be performed at 70°C for 48 h.

3.1.10 Sectioning and Post-staining

1. Cut thin sections (70–80 nm) with an ultramicrotome using a diamond knife and place them on a 200 mesh copper grid.
2. Stain the sections with aqueous uranyl acetate (20 min) followed by lead citrate (2 min) (*see Note 6*) [63].
3. The sections are now ready for imaging in an electron microscope.

3.2 Preparation of Microbial Cells for Visualization by Negative Staining

Negative staining has been employed to visualize electron-transparent hydrocarbon inclusions in hydrocarbon-grown bacteria. A general protocol using staining with phosphotungstic acid by the drop-by-drop method has been described here:

1. Obtain formvar carbon film-coated copper EM grids with medical tweezers with clamping ring, putting the carbon film side up on a clean glass microscope slide, and place the slide on a clean filter paper in a petri dish and cover it.
2. Place ~3 µL of the cell sample on the EM grid carbon film side and incubate for 3–5 min.
3. Remove excess solution by gently touching the edge of the grid with filter paper wicks.
4. Wash the grid by briefly placing the surface of the grid with a drop (~35 µL) of deionized water on Parafilm and then blot with filter paper to remove the excess solution. The touching and blotting steps are to be performed quickly three times, each with a clean drop of deionized water.
5. Stain the grid immediately with 1.5% (w/v) phosphotungstic acid for 1 min and blot the extra solution from the edge of the grid using filter paper.
6. Subsequently, a thin film of this mixture is allowed to air-dry. Image the grid in EM or store it in a grid storage box for future imaging.

3.3 Preparation of Microbial Cell Samples for High-Pressure Freezing–Freeze Substitution (HPF–FS)

1. For high-pressure freezing, resuspend the microbial cells in hexadecane or 2% agarose as filler and introduce the mixture in 100 µm deep membrane carriers. Freeze the cells in a Leica EMPACT2-RTS high-pressure freezer.
2. Transfer the rapidly frozen samples, under liquid nitrogen, to cryotubes containing the freeze substitution medium.
3. Place the cryotubes in the freeze substitution apparatus (automatic FS system 1, AFS-1, Leica) with a temperature maintained at –90°C.

4. Let the samples sit at this temperature for 48 h, and during this time, the solvent mixture slowly replaces the cellular water.
5. Slowly warm up the temperature of the samples (5°C per hour) until it reaches -30°C. Hold at this point for 3 h followed by increase to 0°C (in increments of 5°C per hour).
6. Wash the samples three times with pure acetone on ice and incubate with increasing epoxy/acetone mixture, each step for 2 h.
7. Infiltrate with pure epon overnight, followed by polymerization.

3.3.1 Quick Freeze Substitution Method: Preparation of Microbial Cell Samples for High-Pressure Freezing–Quick Freeze Substitution (HPF–QFS) (see **Notes 7–10)**

This protocol is an improvement over the traditional time-consuming protocol and requires only basic laboratory tools. The results with this method have been found to be similar to those with traditional method [62]:

1. Place a modular heating block (with holes) in a foam box filled with liquid nitrogen.
2. Place a Type T thermocouple temperature probe connected to a data logger in one of the holes.
3. Then add the frozen samples at the liquid-nitrogen temperature. Start the datalogger.
4. Next, pour out the liquid nitrogen from the foam box and rotate the dry block heater with the samples at 100 rpm so that the cryotubes are horizontal. In around 2 h, the samples should have reached 0°C.
5. Remove the samples from the foam box and allow to warm to room temperature on a rocker. Stop the datalogger at this point.
6. Rinse out the fixative with pure acetone and continue with resin infiltration and embedding.

3.4 Diaminobenzidine (DAB) Photoconversion [21, 59]

1. Harvest the cell suspension by centrifugation at 13,000 rpm for 5 min and resuspend in the same volume of the fluorescent staining buffer (Bodipy FL C12).
2. Incubate in the dark, on ice for 30 min.
3. After staining, wash the cells three times in PBS buffer.
4. Fix the washed cells in primary fixative at 4°C for 3 days. Rinse again three times in PBS for 10 min.
5. At this stage, the cells can be embedded in 3.5% (w/v) agarose, sections of about 200 nm cut with a razor blade, followed by overnight fixation in 2% (w/v) paraformaldehyde in PBS or cell suspension can be used as such.
6. Preincubate the washed sections or the cell suspensions in prechilled 0.5 mg/mL DAB solution for 30 min (see **Note 11**).

7. Photoconvert the microbial cells for 1.5 h using a conventional fluorescence microscope with a fluorescein filter setting, a 50 W mercury lamp, and a 10 X objective.
8. Add fresh DAB solution every 15 min.
9. Monitor the development of the brown DAB reaction product. Excise those agarose sections and rinse three times in PBS for 10 min.
10. Postfix for 30 min in 1% (w/v) OsO₄ in PBS. Wash the fixed sections/cells in PBS again and use for TEM preparation (dehydration, resin infiltration, embedding, and polymerization) as described in Sects. 3.1.7, 3.1.8, 3.1.9, and 3.1.10.

4 Notes

1. Addition of calcium chloride (1–3 mM) to the glutaraldehyde fixation can minimize lipid loss during dehydration steps.
2. The formula for relative centrifugal force is $RCF = 11.2r(RPM/1,000)^2$, where r = radius in centimeters and RPM = revolutions per minute.
3. Glass pipettes can be used but they should be fire-polished to prevent the release of small chips of glass in the specimen. Such glass chips will damage the knives used in ultramicrotomy.
4. Acetonitrile can be used instead of propylene oxide due to carcinogenic nature of propylene oxide.
5. Do not shake the tube containing the resin components too vigorously or bubbles will be introduced that will interfere with the embedding. The few bubbles that form during the inversion process will rise to the surface and not pose a problem.
6. The Reynolds' lead citrate will react with carbon dioxide in the air to form a lead carbonate precipitate, so it must be stored in a tightly sealed volumetric flask.
7. It is important to note that for high-pressure freezing methods to work most effectively, the high-pressure frozen material should be removed from the freezer specimen cups before resin infiltration.
8. While using cryotubes with O-ring seal, it is a good idea to do a test run on the cryovials filled with acetone only to make sure they do not leak before using them with fixatives.
9. Liquid nitrogen expands about 700-fold in going from the liquid to gaseous state. Even a small amount of liquid sealed in a cryotube could cause it to explode. It is imperative that liquid nitrogen is not sealed in a cryotube.

10. It is best to have the lids of the cryotubes at room temperature just before putting them on, so the O-ring is pliable and gives a good seal.
11. The DAB solution must be made fresh and should be pre-chilled. The low temperature maintains high oxygen content and supports effective and specific DAB polymerization.

References

1. Ladygina N, Deyukhina EG, Veinshtein MB (2006) A review on microbial synthesis of hydrocarbons. *Process Biochem* 41:1001–1014
2. Head I, Aitken C, Gray N et al (2010) Hydrocarbon degradation in petroleum reservoirs. In: Timmis K (ed) *Handbook of hydrocarbon and lipid microbiology*. Springer, Berlin/Heidelberg
3. Sierra-Garcia I, de Oliveira V (2013) Microbial hydrocarbon degradation: efforts to understand biodegradation in petroleum reservoirs. In: Chamy R (ed) *Biodegradation – engineering and technology*. InTech, ISBN: 978-953-51-1153-5, doi:10.5772/55920
4. Wenger L, Davis C, Isaksen G (2002) Multiple controls on petroleum biodegradation and impact on oil quality. In: *Society for petroleum engineers (SPE) reservoir evaluation and engineering*, pp 375–383
5. Roling W, Head I, Larter S (2003) The microbiology of hydrocarbon degradation in subsurface petroleum reservoirs: perspectives and prospects. *Res Microbiol* 154:321–328
6. Atlas R, Bartha R (1993) *Microbial ecology - fundamentals and applications*. Benjamin-Cummings, Redwood City
7. Atlas R (1981) Microbial degradation of petroleum hydrocarbons: an environmental perspective. *Microbiol Rev* 45(1):180–209
8. Van Hamme J, Singh A, Ward O (2003) Recent advances in petroleum microbiology. *Microbiol Mol Biol Rev* 67(4):503–549
9. Muthuswamy S, Binupriya A, Baik S, Yun S (2008) Biodegradation of crude oil by individual bacterial strains and a mixed bacterial consortium isolated from hydrocarbon contaminated areas. *Clean* 36(1):92–96
10. Martins L, Piexoto R (2012) Biodegradation of petroleum hydrocarbons in hypersaline environments. *Braz J Microbiol* 43(3):865–872
11. Hazen T, Dubinsky E, De Santis T, Andersen G et al (2010) Deep-sea oil plume enriches indigenous oil-degrading bacteria. *Science* 330(6001):204–208
12. Baelum J, Borglin S, Chakraborty R, Fortney J et al (2012) Deep-sea bacteria enriched by oil and dispersant from the deepwater horizon spill. *Environ Microbiol* 14(9):2405–2416
13. Biological Agents. <http://www2.epa.gov/emergency-response/biological-agents>. Accessed 24 Nov 2014
14. Kostka J, Prakash O, Overholt W, Green S et al (2011) Hydrocarbon degrading bacteria and the bacterial community response in Gulf of Mexico beach sands impacted by the deepwater horizon oil spill. *Appl Environ Microbiol* 77(22):7962
15. Scott C, Finnerty W (1976) A comparative analysis of the ultrastructure of hydrocarbon – oxidizing microorganisms. *J Gen Microbiol* 94:342–350
16. Pinzon N, Aukema K, Gralnick J et al (2011) Nile red detection of bacterial hydrocarbons and ketones in a high throughput format. *MBio* 2(4):e00109-11. doi:10.1128/mBio.00109-11
17. Singer M, Tyler S, Finnerty W (1985) Growth of *Acinetobacter* sp. strain HO1-N on n-hexadecanol: physiological and ultrastructural characteristics. *J Bacteriol* 162(1):162
18. Alvarez H, Steinbuchel A (2002) Triacylglycerols in prokaryotic microorganisms. *Appl Microbiol Biotechnol* 60:367–376
19. Waltermann M, Steinbuchel A (2005) Neutral lipid bodies in prokaryotes: recent insights into structure, formation and relationship to eukaryotic lipid depots. *J Bacteriol* 187(11):3607
20. Marin M, Pedregosa A, Laborda F (1996) Emulsifier production and microscopical study of emulsions and biofilms formed by the hydrocarbon-utilizing bacteria *Acinetobacter calcoaceticus* MM5. *Appl Microbiol Biotechnol* 44:660–667
21. Waltermann M, Hinz A, Robenek H et al (2005) Mechanism of lipid body formation in

- prokaryotes: how bacteria fatten up. *Mol Microbiol* 55(3):750–763
22. Meng X, Yang J, Xu X, Zhang L, Nie Q, Xian M (2009) Biodiesel production from oleaginous microorganisms. *Renew Energy* 34:1–5
 23. U.S. Bioenergy Statistics. <http://www.ers.usda.gov/data-products/us-bioenergy-statistics>. Accessed 10 Oct 2014
 24. Shi S, Valle-Rodriguez J, Siewers V, Nielsen J (2011) Prospects for microbial biodiesel production. *Biotechnol J* 6:277–285
 25. Suzuki R, Ito N, Uno Y, Nishii I et al (2013) Transformation of lipid bodies related to hydrocarbon accumulation in a green alga, *Botryococcus braunii* (Race B). *PLoS One* 8(12), e81626. doi:10.1371/journal.pone.0081626
 26. Davies S, Whittenbury R (1970) Fine structure of methane and other hydrocarbon-utilizing bacteria. *J Gen Microbiol* 61:227–232
 27. Kennedy R, Finnerty W, Sudarsanan K, Young R (1974) Microbial assimilation of hydrocarbons. I. The fine-structure of a hydrocarbon oxidizing *Acinetobacter* sp. *Arch Microbiol* 102:75–83
 28. Alvarez H, Mayer F, Fabritius D, Steinbüchel A (1996) Formation of intracytoplasmic lipid inclusions by *Rhodococcus opacus* strain PD630. *Arch Microbiol* 165(6):377–386
 29. Diestra E, Esteve I, Burnat M, Maldonado J, Sole A (2007) Isolation and characterization of a heterotrophic bacterium able to grow in different environmental stress conditions, including crude oil and heavy metals. In: Méndez-Vilas A (ed) Communicating current research and educational topics and trends in applied microbiology. Formex, Badajoz
 30. Osumi M (2012) Visualization of yeast cells by electron microscopy. *J Electron Microscop* 61(6):343–365
 31. Li Z (ed) (2002) Industrial application of electron microscopy. CRC Press, Boca Raton, p 362
 32. Wigglesworth V (1975) Lipid staining for the electron microscope: a new method. *J Cell Sci* 19:425–437
 33. Trent J (1984) Ruthenium tetroxide staining of polymers: new preparative methods for electron microscopy. *Macromolecules* 17:2930–2931
 34. Khandpur A, Macosko C, Bates F (1995) Transmission electron microscopy of saturated hydrocarbon block copolymers. *J Polym Sci B Polym Phys* 33:247–252
 35. Richter H, Sleytr U (1971) Fettextraktion bei -78°C : nachweis im Gefrieratzbild. *Z Naturforsch* 26b:470–473
 36. Meyer H, Winkelmann H (1970) Die Darstellung von lipiden bei der gefrieratzpreparation und ihre beziehung zur strukturanalyse biologischer membranen. *Exp Pathol* 4:47–59
 37. Moor H, Muhlethaler K (1963) Fine structure in frozen etched yeast cells. *J Cell Biol* 17:609–628
 38. Meyer H, Richter W (2001) Freeze-fracture studies on lipids and membranes. *Micron* 32:615–644
 39. Scott C, Finnerty W (1976) Characterization of intracytoplasmic hydrocarbon inclusions from the hydrocarbon-oxidizing *Acinetobacter* Species HO1-N. *J Bacteriol* 127(1):481–489
 40. Ishige T, Tani A, Takabe K, Kawasaki K et al (2002) Wax ester production from n-Alkanes by *Acinetobacter* sp. strain M-1: ultrastructure of cellular inclusions and role of acyl coenzyme A reductase. *Appl Environ Microbiol* 68(3):1192–1195
 41. Bleck C, Merz A, Gutierrez M, Alther P et al (2010) Comparison of different methods for thin section EM analysis of *Mycobacterium smegmatis*. *J Microsc* 237:23–28
 42. Fujimoto K (1995) Freeze-fracture replica electron microscopy combined with SDS digestion for cytochemical labeling of integral membrane proteins - application to the immunogold labeling of intercellular junctional complexes. *J Cell Sci* 108:3443–3449
 43. Severs N (1995) Freeze-fracture cytochemistry: an explanatory survey of methods. In: Severs N, Shotton D (eds) Rapid freezing, freeze fracture, and deep etching. Wiley-Liss, New York, pp 173–208
 44. Robenek H, Severs N (2008) Recent advances in freeze-fracture electron microscopy: the replica immunolabeling technique. *Biol Proced Online* 10:9–19
 45. Scott C, Makula S, Finnerty W (1976) Isolation and characterization of membranes from a hydrocarbon-oxidizing *Acinetobacter* sp. *J Bacteriol* 127(1):469–480
 46. Kellenberger E, Johansen R, Maeder M, Bohrmann B et al (1992) Artefacts and morphological changes during chemical fixation. *J Microsc* 168:181–201
 47. Mc Donald K, Auer M (2006) High-pressure freezing, cellular tomography, and structural cell biology. *Biotechniques* 41(2):137, 139, 141
 48. Djaczenko W, Muller M, Benedetto A (1990) Ultra-rapid high pressure freezing in high resolution EM of cell-cell and cell-substrate interactions. *Cell Biol Int Rep* 14

49. Dubochet J (1995) High-pressure freezing for cryoelectron microscopy. *Trends Cell Biol* 5 (9):366–368
50. Hurbain I, Sachse M (2011) The future is cold: cryo-preparation methods for transmission electron microscopy of cells. *Biol Cell* 103:405–420
51. Paul T, Beveridge T (1994) Preservation of surface lipids and determination of ultrastructure of *Mycobacterium kansasii* by freeze substitution. *Infect Immun* 62(5):1542–1550
52. Al-Amoudi A, Chang J, Leforestier A, McDowall A et al (2004) Cryo-electron microscopy of vitreous section. *EMBO J* 23 (18):3583–3588
53. Comolli L, Kundmann M, Downing K (2006) Characterization of intact subcellular bodies in whole bacteria by cryo-electron tomography and spectroscopic imaging. *J Microsc* 223:40–52
54. Thomson N, Channon K, Mokhtar N, Staniewicz L et al (2011) Imaging internal features of whole, unfixed bacteria. *Scanning* 33(2):59–68
55. (2010) Probes for lipids and membranes. In: *The molecular probes® handbook: a guide to fluorescent probes and labeling technologies*, 11th edn. <http://www.lifetechnologies.com/us/en/home/references/molecular-probes-the-handbook/probes-for-lipids-and-membranes.html>
56. Chen W, Zhang C, Song L, Sommerfeld M, Hu Q (2009) A high throughput Nile red method for quantitative measurement of neutral lipids in microalgae. *J Microbiol Methods* 77:41–47
57. Elle I, Olsen L, Pultz D, Rødkær S, Færgeman N (2010) Something worth dyeing for: molecular tools for the dissection of lipid metabolism in *Caenorhabditis elegans*. *FEBS Lett* 584:2183–2193
58. Govender T, Ramanna L, Bux R (2012) BOD-IPY staining, an alternative to the Nile Red fluorescence method for the evaluation of intracellular lipids in microalgae. *Bioresour Technol* 114:507–511
59. Dantuma N, Pijnenburg M, Diederens J, Van der Horst D (1998) Electron microscopic visualization of receptor-mediated endocytosis of DiI-labeled lipoproteins by diaminobenzidine photoconversion. *J Histochem Cytochem* 46 (9):1085–1089
60. Cortese K, Diaspro A, Tacchetti C (2009) Advanced correlative light/electron microscopy: current methods and new developments using Tokuyasu cryosections. *J Histochem Cytochem* 57(12):1103–1112
61. Staubli W (1963) A new embedding technique for electron microscopy, combining a water soluble epoxy resin (Durcupan) with water insoluble Araldite. *J Cell Biol* 16:197–199
62. Mc Donald K, Webb R (2011) Freeze substitution in 3 hours or less. *J Microsc* 243 (3):227–233
63. Reynolds ES (1963) The use of lead citrate at high pH as an electron-opaque stain for electron microscopy. *J Cell Biol* 17:208